Journal of Plastic, Reconstructive & Aesthetic Surgery (2019) 72, 1355–1362

JPRAS
An International Journal of Surgical Reconstruction
www.JPRASurg.com

Hyaluronic acid-cross-linked filler stimulates collagen type 1 and elastic fiber synthesis in skin through the TGF-β/Smad signaling pathway in a nude mouse model

Yingfang Fan[a], **Tae-Hyun Choi**[a,b], **Jee-Hyeok Chung**[c], **Yoon-Kyung Jeon**[d], **Sukwha Kim**[a,b,*]

[a] *Department of Plastic and Reconstructive Surgery, Seoul National University College of Medicine, 101 Daehak-ro, Jongno-gu, Seoul 03080, South Korea*
[b] *Department of Plastic and Reconstructive Surgery, Institute of Human-Environment Interface Biology, Seoul National University College of Medicine, Seoul, South Korea*
[c] *Department of Plastic and Reconstructive Surgery, MyongJi Hospital, 55, Hwasu-ro 14beon-gil, Deokyang-gu, Goyang-si, Gyeonggi-do 10475, South Korea*
[d] *Department of Pathology, Seoul National University College of Medicine, Seoul, South Korea*

Received 27 September 2018; accepted 30 March 2019

KEYWORDS
HAc-nano-HAp;
HAc-micro-HAp;
Dermal filler;
TGF-β/Smad pathway;
Collagen type 1;
Elastic fiber

Summary Compared to pure hyaluronic acid filler, cross-linked hyaluronic acid (HAc) exhibits superior biocompatibility and longevity as a dermal filler. We previously developed composite HAc-hydroxyapatite (HAp) fillers. Herein, we systematically compared the protein-level increase and gene expression between HAc-micro-HAp and HAc-nano-HAp in mice and determined the mechanisms underlying the biological responses to HAc and HAp.

Five-week-old female BALB/c-nude mice were classified into five groups: normal skin, Radiesse, Restylane, HAc-nano-HAp, and HAc-micro-HAp. Fillers (200 μl) were injected to evenly fill the back of mice. Skin biopsies were performed to investigate collagen and elastic fiber synthesis after filler injections. Western blot analysis, real-time polymerase chain reaction analysis, and immunohistochemistry were performed to investigate protein and gene expression changes. Organ (liver, lung, spleen, and kidney) toxicity of HAc-nano-HAp was determined by hematoxylin and eosin staining after 12 weeks. Protein and gene expression analyses indicated that, compared with pure fillers, HAc-nano-HAp and HAc-micro-HAp hydrogels preferentially promoted collagen and elastic fiber formation through the TGF-β pathway. The composite fillers also exhibited no evidence of organ toxicity.

* Corresponding author at: Department of Plastic and Reconstructive Surgery, Seoul National University College of Medicine, 101 Daehak-ro, Jongno-gu, Seoul 03080, South Korea.
E-mail address: kimsw@snu.ac.kr (S. Kim).

https://doi.org/10.1016/j.bjps.2019.03.032
1748-6815/© 2019 British Association of Plastic, Reconstructive and Aesthetic Surgeons. Published by Elsevier Ltd. All rights reserved.

HAc–HAp filler might play an important role in collagen and elastic fiber regeneration. HAc filler stimulates collagen type 1 and elastic fiber synthesis through the TGF-β/Smad pathway. The role of HAc–HAp composite fillers in photoaging in animal models and their effects on skin, including elasticity and tensile strength, should be investigated.
© 2019 British Association of Plastic, Reconstructive and Aesthetic Surgeons. Published by Elsevier Ltd. All rights reserved.

Introduction

Skin aging and laxity are associated with dermal matrix alterations such as decreases in collagen levels and elastic fibers and atrophy.[1-3] However, in the past decade, considerable advances have been made in the field of esthetic medicine with regard to the use of dermal fillers to improve skin defects.[2-5]

The most commonly used material for dermal filler is hyaluronic acid (HAc).[6] HAc filler exhibits superior bioactivity and biocompatibility properties to other fillers.[7] Cross-linked HAc filler stimulates fibroblasts to produce collagen fiber through the TGF-β/Smad pathway,[1,3,8] although the precise pathway is debatable. In the dermal microenvironment, collagen stimulation is associated with enhanced expression of type II TGF-β receptor, the major regulator of type I procollagen synthesis in human skin.[8-10] HAc facilitates interaction between CD44 and EGFR, thus promoting MAPK/ERK phosphorylation and inducing TGF-β1-dependent fibroblast proliferation.[11] HAc can also promote elastic fiber growth.[1,3] For example, TGF-β stimulates the expression of many genes necessary for elastic fiber production, including elastin and fibrillin.[12,13] However, despite their many advantages, HAc-based dermal fillers often last for only a few months in vivo owing to rapid enzymatic degradation.[5]

We previously developed two kinds of HAc-hydroxyapatite (HAp) composite fillers, HAc-micro-HAp and HAc-nano-HAp, and demonstrated that a cross-linked HAc–HAp filler, which has better longevity than pure HAc fillers, promotes collagen regeneration in a nude mouse model.[14] In this study, we systematically compared the biocompatibility, and specific protein and gene expression changes between HAc-micro-HAp, HAc-nano-HAp, and pure fillers in mice to determine the mechanisms underlying the biological responses to HAc and HAp.

Materials and methods

HAc–HAp composite filler preparation

Composite filler preparation

To fabricate the HAc–HAp composite filler, pure HAc with molecular weight of 1.8–2.5 MDa was prepared (BioMed, Seoul, Korea). All composite hydrogels were homogenized at 7000 rpm for 5 min and autoclaved at 121 °C for 30 min to prepare the gel particles for injection through a needle. As the pure HAc filler was prepared using the cross-linker 1,4-butanediol diglycidyl ether (BDDE), the same cross-linking system was used to prepare the HAc–HAp composite filler.

HAc-nano-HAp composite hydrogel

HAc (10 w/v%) in 0.2 N NaOH solution was cross-linked using the cross-linker BDDE for 12 h at 40 °C. The cross-linked hydrogel was dialyzed and fully swollen in distilled water at room temperature. It was then immersed in a solution of 3 w/v% $CaCl_2$ and a molar ratio of 1.67 H_3PO_4 for 2 h. Subsequently, it was dipped in 15% NH_4OH solution for 30 min to precipitate 30 wt% of nano-HAp within the hydrogel. The average size of nano-HAp particles was 200 nm.

HAc-micro-HAp composite hydrogel

Prior to cross-linking, HAp microspheres were prepared by spray drying a solution consisting of HAp powder, PVB, and KD6, followed by heat treatment at 500 °C for 2 h and 1200 °C for 2 h. HAp microspheres (30 vol%) with an average size of 20 μm were homogeneously mixed into the 10 w/v% of HAc solution with BDDE cross-linker in 0.2 N NaOH. The mixture was sealed and maintained at 40 °C for 12 h to allow gelation, followed by washing and swelling in PBS (refreshed daily) at room temperature.

Animal experiments

We obtained 24 female, 5-week-old BALB/c nude mice from ORIENT BIO Inc. (Seongnam, Korea). Mice were fed a standard diet. After 1 week of acclimatization, the mice were injected, using a 30-guage needle, with 200 μl of HAp (Radiesse, Raleigh, North Carolina), HAc (Restylane, Uppsala, Sweden), HAc-nano-HAp, or HAc-micro-HAp between the panniculus adiposus layer and the panniculus carnosus of the back skin. Four injections were administered per mouse ($n = 20$). Uninjected mice served as controls ($n = 4$). At weeks 1, 4, 8, and 12, five skin biopsies were collected and cut into 3 pieces for real-time polymerase chain reaction (PCR) amplification, western blot analyses, and histological examination. These experiments were approved by the Institutional Animal Care and Use Committee of the Seoul National University (IACUC Protocol No. 15-0075).

Real-time PCR

The remaining skin tissues (*i.e.*, the epidermis, dermis, and panniculus adiposus layer), following filler removal, were frozen at −80 °C. RNA was isolated from frozen tissues (50 mg), using TRIzol reagent (500 ml) (Molecular Research Center, Cincinnati, OH, USA), resuspended in RNase-free water, and quantified in a UV spectrophotometer. cDNA was prepared from 1 mg total RNA using TOPscript™ RT DryMIX (Enzynomics, Inc., Daejeon, Korea) according to manufacturer's instruction. Real-time PCR was performed in an ABI 7500 (Applied Biosystems, Inc., Foster City, CA, USA) with SYBR Premix Ex Taq™ (TaKaRa, Otsu, Japan) as follows: 15 min at 95 °C, followed by 40 cycles of 10 s at 95 °C, 15 s at 60 °C, and 30 s at 72 °C. The average threshold cycle for each gene was determined from triplicate reactions. The

Table 1 Target genes used for real-time PCR.

List of genes
Procollagen-sense
Procollagen-antisense
EGFR-sense
EGFR-antisense
Smad2-sense
Smad2-antisense
Smad3-sense
Smad3-antisense
Elastin-sense
Elastin-antisense
Fibrillin-sense
Fibrillin-antisense
ß-Actin-sense
ß-Actin-antisense

EGFR, Epidermal growth factor receptor.

gene expression levels were normalized to that of ß-actin. The target genes were *Egfr, Smad2, Smad3*, procollagen, elastin, and fibrillin (Table 1).

Western blot analysis

Frozen, filler-free skin biopsy samples were homogenized in lysis buffer and centrifuged at 16,873 g for 10 min, and the supernatants were used for western blot analysis. The primary antibodies were as follows: anti-mouse collagen type 1 (Abcam), anti-EGFR (Abcam), anti-TGF-β (Abcam), anti-Smad2/3 (Cell Signaling Technology (CST), Danvers, MA, USA), anti-MAPK (Erk1/2) (CST), anti-phosphorylated MAPK (Erk1/2) (CST), anti-Smad7 (Santa Cruz Biotechnology, Dallas, TX, USA), and anti-β-actin (Abcam). The secondary antibody was anti-rabbit IgG (Abcam). Proteins were visualized by enhanced chemiluminescence (Thermo Fisher Scientific, Rockford, IL, USA). Western blots were performed thrice for each protein. Data were quantified by band-intensity densitometric analysis (ImageJ).

Histological observations

The injected skin biopsies, measuring 1 cm $\times$ 1 cm, were extracted and fixed in 10% formaldehyde for 24 h, then embedded in paraffin, and sectioned (6 μm). The sections were stained with Verhoeff–Van Gieson to visualize the production of elastin. Representative images were analyzed using image analysis software (ImageJ; National Institutes of Health, Bethesda, MD, USA) (Leica QWin V3; Leica Microsystems Cambridge, England, UK). To determine the organ (liver, lung, spleen, and kidney) immunogenicity of HAc-nano-HAp nanoparticles, hematoxylin and eosin staining was performed after 12 weeks.

Immunohistochemical analysis

Tissue sections were cut and placed on microscope slides. The Discovery XT-automated immunohistochemistry stainer (Ventana Medical Systems, Inc., Tucson, AZ, USA) was used to stain slides, and the Ventana Chromo Map Kit was used for detection. The tissue sections were deparaffinized, and a CC1 standard [buffer containing Tris, borate, and ethylenediaminetetraacetic acid, pH 8.4] was used to retrieve the antigen. Inhibitor D (3% H_2O_2, endogenous peroxidase) was submerged in for 4 min at 37 °C. The slides were incubated with 1:3000 antitropoelastin (Abcam, Cambridge, MA, USA) for 32 min at 37 °C, followed by incubation with OmniMap anti-rabbit horseradish peroxidase as a secondary antibody for 20 min at 37 °C. The other slides were incubated with 1:500 vimentin (Abcam) as the primary antibody for 32 min at 37 °C. The slides were incubated in diaminobenzidine with H_2O_2 as the substrate for 8 min at 37 °C, followed by counterstaining with bluing hematoxylin reagent at 37 °C. Tris buffer (pH 7.6) was used as the washing solution. Each slide was measured at five locations, and the mean values were compared. The stained slides were evaluated using image analysis software (Leica QWin V3 and Leica Microsystems CMS GmbH, Wetzlar, Germany).

Statistical analysis

All data were analyzed by the Kruskal–Wallis test, with IBM SPSS software version 20.0 (Armonk, NY, USA). Step-up Mann–Whitney tests were performed with a multiple comparison adjustment. A P-value <0.05 was considered statistically significant.

Results

Dermal collagen and elastic fiber formation after Radiesse and HAc-micro-HAp treatment

Real-time PCR and western blot analysis

To detect gene expression and protein level, real-time PCR and western blot were performed. As assessed by real-time PCR after 4 and 12 weeks (Figure 1), the *EGFR, Smad2*, procollagen, elastin, and fibrillin mRNA expression levels exhibited similar patterns. The procollagen levels were significantly higher in the HAc-micro-HAp group than in the Radiesse group ($P < 0.005$). The *Smad2* and fibrillin levels of the HAc-micro-HAp group were significantly higher than those of the Radiesse group ($P < 0.05$), whereas the Smad3 levels were significantly lower ($P < 0.05$). No significant differences in the expression of any gene were observed between groups at week 12, at which time the gene expression levels decreased. Protein expression was visualized by western blotting at 12 weeks after filler injection (Supplementary Figure 1). The HAc-micro-HAp groups showed a similar pattern for TGF-β, EGFR, p-MAPK, Smad2/3, and collagen type 1 expression, whereas the Radiesse group did not. The level of P-MAPK in the Radiesse group did not change significantly compared with that in the normal group. Expression of Smad7, an inhibitor of the TGF-β/Smad signaling pathway, was not negatively correlated with Smad2/3 protein expression in either group ($P < 0.05$).

Histological and immunohistochemical analysis

Supplementary Figure 2(A) and (B) shows the results of Verhoeff–Van Gieson staining. Elastic fiber (black area in the

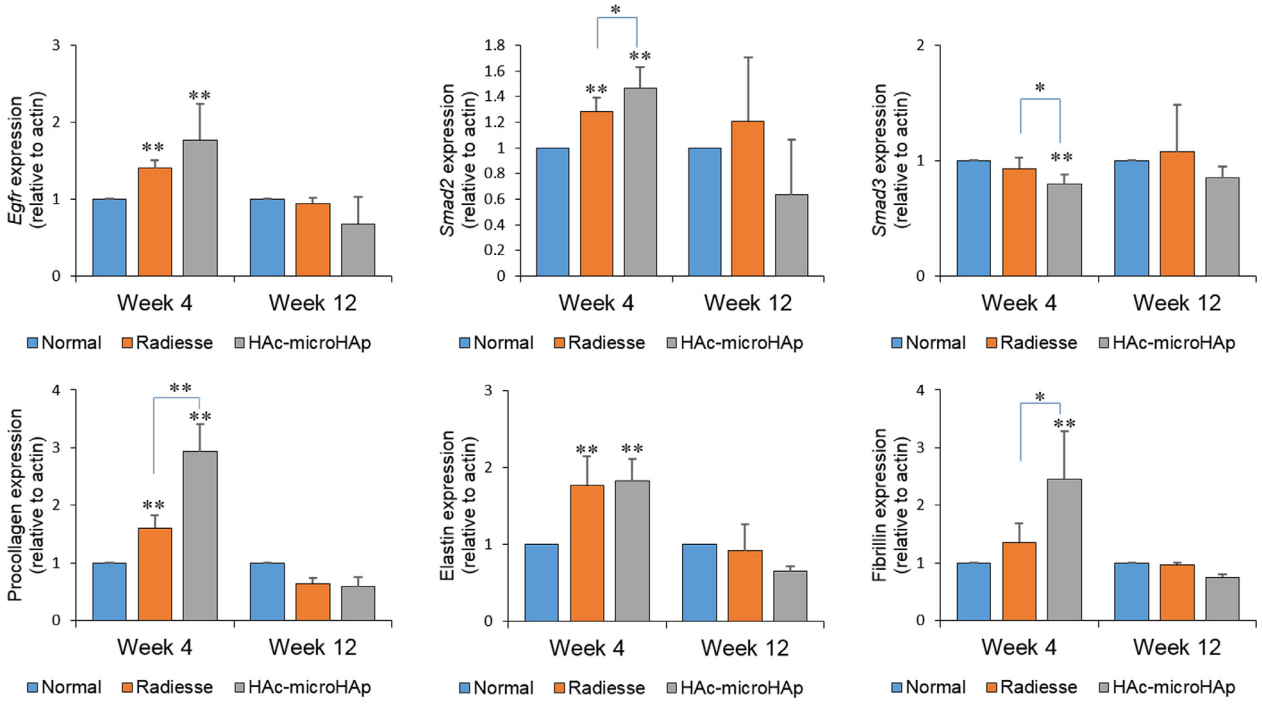

Figure 1 Real-time PCR was performed after 4 and 12 weeks. The procollagen levels were significantly higher in the HAc-micro-HAp group than in the Radiesse group (**$P < 0.005$). The *Smad2* and fibrillin levels of the HAc-micro-HAp group were significantly higher than those of the Radiesse group (*$P < 0.05$), whereas the Smad3 levels were significantly lower (*$P < 0.05$). **Statistically significant when compared with the normal group ($P < 0.005$).

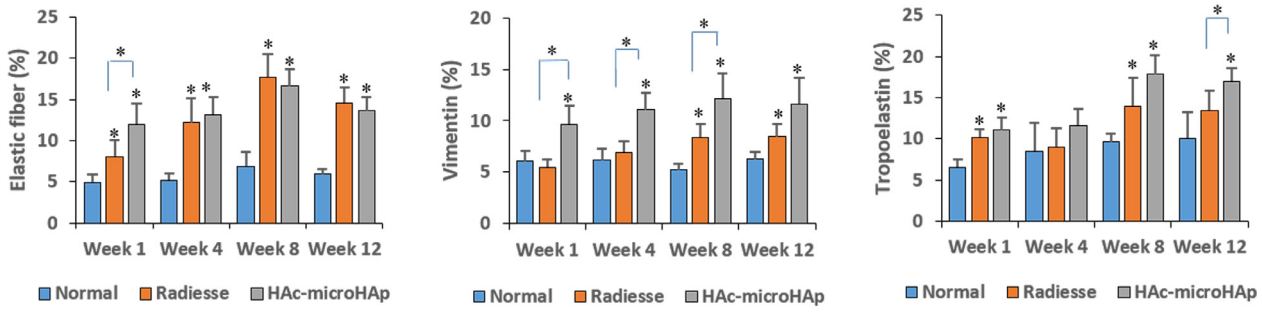

Figure 2 Collagen and elastic fiber formation in the Radiesse and HAc-micro-HAp groups. *Statistically significant when compared with the normal group ($P < 0.05$); statistically significant difference between the Radiesse and HAc-micro-HAp groups ($P < 0.05$).

dermis) was measured as the mean value of 5 different fields on the same slide. A significant increase in the dermal elastic fiber was observed at weeks 1, 4, 8, and 12 after the filler injections. The elastic fiber area of the HAc-micro-HAp group was significantly larger than that of the Radiesse group at week 1 ($P < 0.05$, Figure 2). Immunohistochemistry analysis of the fibroblast marker vimentin (Supplementary Figure 2(C) and (D)) showed initial increased levels in the HAc-micro-HAp group, with significant increases after 1, 4, and 8 weeks ($P < 0.05$, Figure 2). The tropoelastin levels (Supplementary Figure 2(E) and (F)) of the Radiesse and HAc-micro-HAp groups increased significantly at weeks 1 and 8. At week 12, the tropoelastin levels in the HAc-micro-HAp group were significantly higher than those in the Radiesse group ($P < 0.05$, Figure 2).

Dermal collagen and elastic fiber formation after Restylane and HAc-Nano-HAp treatment

Real-time PCR and western blot analysis

At week 4, the *Egfr, Smad2*, procollagen, elastin, and fibrillin mRNA expression levels had similar patterns, whereas no significant differences were observed for *Smad3*. The *Egfr* and elastin levels of the HAc-nano-HAp group were significantly higher than those of the Restylane group ($P < 0.005$, Figure 3). No significant differences in the expression of any gene were observed between groups at week 12, at which time the gene expression levels decreased. Western blotting at 12 weeks after filler injections showed that the Restylane and HAc-nano-HAp groups had similar levels of TGF-β, EGFR, p-MAPK, Smad2/3, and collagen type 1

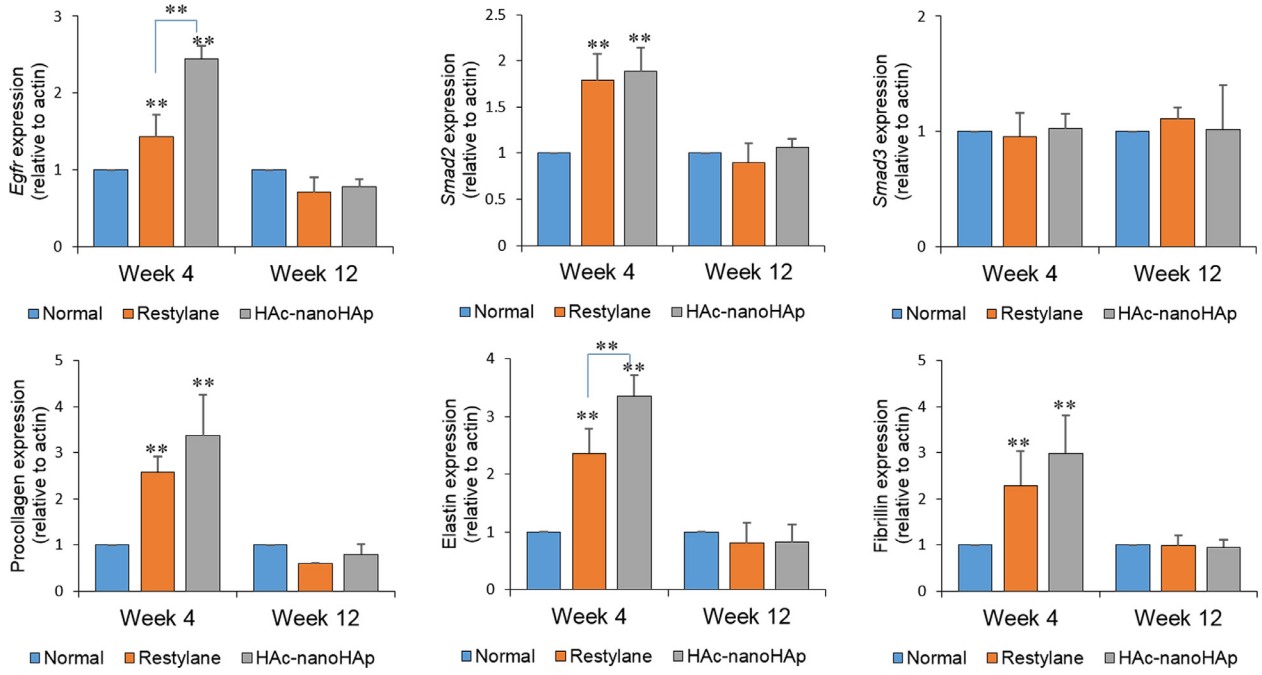

Figure 3 Real-time PCR was performed after 4 and 12 weeks. The *Egfr* and elastin levels of the HAc-nano-HAp group were significantly higher than those of the Restylane group (**$P < 0.005$). **Statistically significant when compared with the normal group ($P < 0.005$).

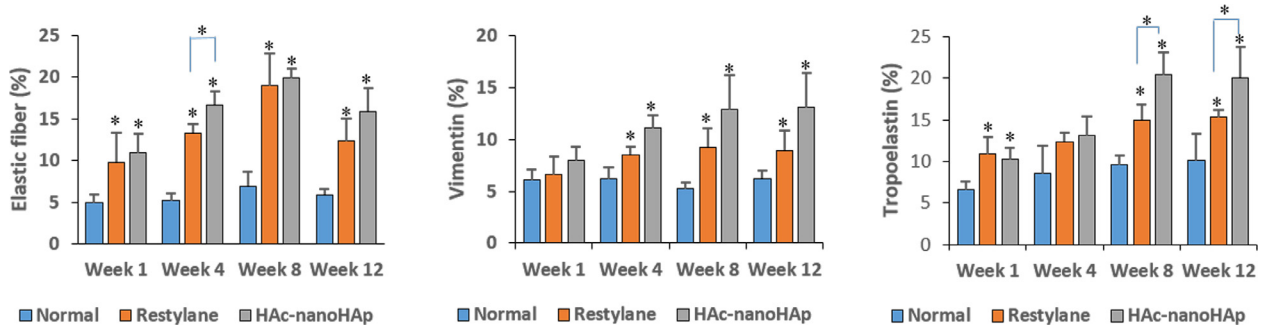

Figure 4 Collagen and elastic fiber formation in the Restylane and HAc-nano-HAp groups. *Statistically significant when compared with the normal group ($P < 0.05$); statistically significant difference between the Restylane and HAc-nano-HAp groups ($P < 0.05$).

(Supplementary Figure 3), although the EGFR, p-MAPK, and collagen type 1 levels of the HAc-nano-HAp group increased significantly compared to those in controls ($P < 0.005$). Smad7 expression was negatively correlated with Smad2/3 protein expression in both groups.

Histological and immunohistochemical analysis

The elastic fiber (Supplementary Figure 4(A) and (B)) area of the HAc-nano-HAp group was significantly larger than that of the Restylane group at week 4 ($P < 0.05$, Figure 4). The vimentin levels (Supplementary Figure 4(C) and (D)) in the Restylane and HAc-nano-HAp groups increased significantly after 4 weeks but did not exhibit additional changes after 8 and 12 weeks ($P < 0.05$, Figure 4). At weeks 1, 4, 8, and 12, a significant increase in the dermal elastic fiber was observed after the filler injections. The tropoelastin levels (Supplementary Figure 4(E) and (F)) of the Restylane and HAc-nano-HAp groups increased significantly at week 1. At weeks 8 and 12, the tropoelastin levels of the HAc-nano-HAp group were significantly higher than those of the Restylane group, whereas the two filler groups maintained similar tropoelastin levels after 12 weeks ($P < 0.05$, Figure 4).

Nanoparticle safety

The kidney, liver, lung, and spleen were stained with H&E at week 12. H&E staining identified no organ damage, structural malformation, or necrosis. Additionally, no abnormal inflammatory cell infiltration and no abnormal increase in macrophages were observed in any of the organs (Supplementary Figure 5).

Discussion

HAc filler is the most common dermal injection,[3,6,15] with cross-linked HAc fillers (CaHA) effectively increasing

dermal thickness and extracellular matrix components[1,4,16] including collagen and elastic fibers.[17,18] The CaHA Radiesse is highly effective with regard to improving facial contours;[4,19-21] however, its longevity is insufficient owing to its biodegradability.[21] In comparison, we previously demonstrated the longevity of the HAc-HAp composite filler, and its effects on collagen synthesis were demonstrated in a nude mouse model.[14] Imaging and MRI volumetric analyses revealed that the HAc-HAp composite filler had better longevity than pure HAc, with HAc-nano-HAp exhibiting the best stability among the tested groups. In our previous study, at week 8, the collagen areas of the HAc-nano-HAp group had increased significantly and similar collagen levels were maintained after 12 weeks.[14] This effect may be associated with regulation of the TGF-β/Smad pathway.

As growth should therefore be most obvious in the previous stage, here, we analyzed gene expression changes at week 4. The *Egfr, Smad2*, and procollagen mRNA expression levels exhibited similar patterns at week 4, and the procollagen levels were significantly higher in the HAc-micro-HAp group, suggesting the upregulated expression of *Egfr* and *Smad2* promoting collagen synthesis. HAc collagen formation occurs through *Egfr* and *Smad2*. In contrast, *Smad3* expression showed a contrasting pattern to a significant degree. In the extracellular matrix environment, both Smad2 and Smad3 can inhibit increases in the expression of the other.[22] Thus, upregulated expression of *Smad2* promoted *Smad3* degradation. The significant increase in the fibroblast marker vimentin[23,24] in the HAc-micro-HAp group suggested enhanced fibroblast numbers, consistent with the dermal thickness and collagen area findings reported in our previous study. It also supports the hypothesis summarized in Supplementary Figure 6. It is not clear whether Radiesse also induces collagen formation through the TGF-β/Smad pathway. Literature shows that HAp injected into the living bone promotes new bone formation by osteoblasts and osteoclasts;[25] furthermore, the HAp scaffold is similar to the natural bone extracellular matrix and promotes bone regeneration through the BMP/Smad pathway.[26] When injected into soft tissue, HAp also induces new collagen formation by fibroblast activation.[18,25] However, the specific pathway for these effects has not been elucidated.

In addition, upregulated expression of *Egfr* and *Smad2* promoting elastin and fibrillin synthesis further indicated that HAc promotes collagen and elastic fiber formation through similar TGF-β/Smad pathways (Supplementary Figure 6). Cross-linked HAc increases the expression of elastin and fibrillin in elastic fiber through the TGF-β/Smad pathway. Elastic fiber has two distinct components: microfibrils and elastin.[12] Tropoelastin is a precursor of elastin, and fibrillin-1 is a major component of the microfibrils within elastic fibers.[27,28] In the last week of the study, although elastic fiber levels were equivalent between the groups, tropoelastin levels were significantly higher in the composite group. Furthermore, the *Smad2* and fibrillin levels were significantly higher in the HAc-micro-HAp group at week 4. These findings provide direct and indirect evidence that HAc-micro-HAp can promote enhanced elastic fiber formation. The HAc-micro-HAp group proteins exhibited similar patterns of gene expression unlike the Radiesse group (Figure 1). As Radiesse promotes collagen growth by another signaling pathway, elastic fiber growth may be mediated by another pathway as well. Some studies have shown that collagen and elastic fiber formation induced by HAp are associated with their remodeling and production.[21,29]

The Restylane and HAc-nano-HAp groups, which are all HAc-cross-linked groups, upregulated the expression of *Egfr* and *Smad2*, promoting collagen and synthesis and indicating that HAc promotes collagen formation through the TGF-β/Smad signaling pathway. As *Smad3* expression did not change significantly, Smad2 likely plays a primary role in the HAc-induced TGF-β/Smad signaling pathway. Conversely, Smad7, an inhibitor of the TGF-β/Smad pathway,[30] increased in the Restylane group, suggesting that Smad7 and Smad2/3 protein expression was inversely correlated in the Restylane and HAc-nano-HAp groups, further supporting the hypothesis described in Supplementary Figure 6. These results are consistent with changes in gene expression and protein generation, resulting in collagen fiber assembly in skin tissues.

Additionally, the two HAc groups had similar trends with regard to *Egfr, Smad2*, elastin, and fibrillin gene expression further suggested that cross-linked HAc increases the expression of elastin and fibrillin in elastic fiber through the TGF-β/Smad pathway. Although the elastic fiber decreased in all filler groups at week 12, the HAc-nano-HAp group generally exhibited greater increases in elastic fibers than the Restylane group. The formation of elastic fiber is related to TGF-β,[13] which supports our hypothesis that the HAc filler stimulates an elastic fiber increase through the TGF-β/Smad pathway (Supplementary Figure 6).

Nanoparticles with 1–10 nm diameter might stimulate cytotoxicity by direct effects on chromosomes, ribosomes, and membranes.[31] However, HAp nanoparticles of $<$50 nm are nontoxic at the cellular level.[32] The surface morphology of HAc-nano-HAp was analyzed in our previous study, and spherical nanoparticles with a size of 200 nm were obtained.[14] Consistent with this result, immunogenicity analysis by H&E staining of the HAc-nano-HAp nanoparticles (200 nm) indicated no evidence of morphologic damage or inflammatory response.

These data support the hypothesized collagen and elastic fiber mechanism shown in Supplementary Figure 6, whereby the HAc-HAp filler can effectively increase collagen and elastic fibers and enhance the longevity of the filler. The TGF-β/Smad signaling pathway could promote the proliferation of fibroblasts through the induced Smad proteins. Expression levels of the protein Smad2/3 were upregulated, inhibiting the expression of the protein Smad7, further indicating that the TGF-β/Smad signaling pathway is involved in the process of fibroblast formation and promotes collagen formation. The subsequent results validate the hypothesis that HAc-HAp composite filler promotes collagen and elastic fiber regeneration at both the gene and protein levels, resulting in collagen and elastic fiber assembly in the skin tissue.

Conclusion

Compared with pure filler, the HAc-HAp composite filler has lower degradability; therefore, it has better longevity

and biological properties. The HAc–HAp composite filler promotes more collagen and elastic fiber regeneration through the TGF-β/Smad pathway than the currently available pure fillers. Accordingly, this newly formulated HAc–HAp composite filler likely represents a better option for correcting cosmetic problems such as wrinkles. The antiaging effect of the composite filler can last for a long time, and it can help clinicians and patients avoid multiple injections to maintain the skin rejuvenation.

Although there are no organ morphological changes or immune reactions on histology, definitive evidence of material safety and safe cross-linking is needed prior to clinical application. This is the limitation of this study and a potential field of future research.

Further research should focus on the role of HAc–HAp composite fillers in photoaging in animal models, their toxicity, and their effects on the physical properties of the skin, such as elasticity and tensile strength.

Funding

This research was supported by the R&D Program (S2174750) funded by the Small and Medium Business Administration (SMBA, Korea).

Conflicts of interest

None declared.

Ethical approval

These experiments were approved by the Institutional Animal Care and Use Committee of the Seoul National University (IACUC Protocol No. 15-0075).

Supplementary materials

Supplementary material associated with this article can be found, in the online version, at doi:10.1016/j.bjps.2019.03.032.

References

1. Iannitti T, Morales-Medina JC, Coacci A, Palmieri B. Experimental and clinical efficacy of two hyaluronic acid-based compounds of different cross-linkage and composition in the rejuvenation of the skin. *Pharm Res* 2016;**33**:2879–90.
2. Kim ZH, Lee Y, Kim SM, Kim H, Yun CK, Choi YS. A composite dermal filler comprising cross-linked hyaluronic acid and human collagen for tissue reconstruction. *J Microbiol Biotechnol* 2015;**25**:399–406.
3. Paliwal S, Fagien S, Sun X, et al. Skin extracellular matrix stimulation following injection of a hyaluronic acid-based dermal filler in a rat model. *Plast Reconstr Surg* 2014;**134**:1224–33.
4. Loghem JV, Yutskovskaya YA, Philip Werschler W. Calcium hydroxylapatite: over a decade of clinical experience. *J Clin Aesthet Dermatol* 2015;**8**:38–49.
5. Varma DM, Gold GT, Taub PJ, Nicoll SB. Injectable carboxymethylcellulose hydrogels for soft tissue filler applications. *Acta Biomater* 2014;**10**:4996–5004.
6. Redbord KP, Busso M, Hanke CW. Soft-tissue augmentation with hyaluronic acid and calcium hydroxyl apatite fillers. *Dermatol Ther* 2011;**24**:71–81.
7. Beasley KL, Weiss MA, Weiss RA. Hyaluronic acid fillers: a comprehensive review. *Facial Plast Surg* 2009;**25**:86–94.
8. Quan T, Wang F, Shao Y, et al. Enhancing structural support of the dermal microenvironment activates fibroblasts, endothelial cells, and keratinocytes in aged human skin in vivo. *J Invest Dermatol* 2013;**133**:658–67.
9. Quan T, He T, Kang S, Voorhees JJ, Fisher GJ. Solar ultraviolet irradiation reduces collagen in photoaged human skin by blocking transforming growth factor-beta type II receptor/Smad signaling. *Am J Pathol* 2004;**165**:741–51.
10. Son ED, Lee JY, Lee S, et al. Topical application of 17 beta-estradiol increases extracellular matrix protein synthesis by stimulating TGF-beta signaling in aged human skin in vivo. *J Invest Dermatol* 2005;**124**:1149–61.
11. Meran S, Luo DD, Simpson R, et al. Hyaluronan facilitates transforming growth factor-beta 1-dependent proliferation via CD44 and epidermal growth factor receptor interaction. *J Biol Chem* 2011;**286**:17618–30.
12. Kielty CM, Sherratt MJ, Shuttleworth CA. Elastic fibres. *J Cell Sci* 2002;**115**:2817–28.
13. Urban Z, Davis EC. Cutis laxa: intersection of elastic fiber biogenesis, TGF beta signaling, the secretory pathway and metabolism. *Matrix Biol* 2014;**33**:16–22.
14. Jeong S-H, Fan Y-F, Baek J-U, et al. Long-lasting and bioactive hyaluronic acid-hydroxyapatite composite hydrogels for injectable dermal fillers: physical properties and in vivo durability. *J Biomater Appl* 2016;**31**:464–74.
15. Duranti F, Salti G, Bovani B, Calandra M, Rosati ML. Injectable hyaluronic acid gel for soft tissue augmentation. A clinical and histological study. *Dermatol Surg* 1998;**24**:1317–25.
16. Turlier V, Delalleau A, Casas C, et al. Association between collagen production and mechanical stretching in dermal extracellular matrix: in vivo effect of cross-linked hyaluronic acid filler. A randomised, placebo-controlled study. *J Dermatol Sci* 2013;**69**:187–94.
17. Graivier MH, Bass LS, Busso M, Jasin ME, Narins RS, Tzikas TL. Calcium hydroxylapatite (Radiesse) for correction of the mid- and lower face: consensus recommendations. *Plast Reconstr Surg* 2007;**120**:55S–66S.
18. Marmur ES, Phelps R, Goldberg DJ. Clinical, histologic and electron microscopic findings after injection of a calcium hydroxylapatite filler. *J Cosmet Laser Ther* 2004;**6**:223–6.
19. Bernardini FP, Cetinkaya A, Devoto MH, Zambelli A. Calcium hydroxyl-apatite (Radiesse) for the correction of periorbital hollows, dark circles, and lower eyelid bags. *Ophthal Plast Reconstr Surg* 2014;**30**:34–9.
20. Buchanan AG, Holds JB, Vagefi MR, Bidar M, McCann JD, Anderson RL. Anterior filler displacement following injection of calcium hydroxylapatite gel (Radiesse) for anophthalmic orbital volume augmentation. *Ophthal Plast Reconstr Surg* 2012;**28**:335–7.
21. Pavicic T. Complete biodegradable nature of calcium hydroxylapatite after injection for malar enhancement: an MRI study. *Clin Cosmet Investig Dermatol* 2015;**8**:19–25.
22. Li J, Tang X, Chen X. Comparative effects of TGF-β2/Smad2 and TGF-β2/Smad3 signaling pathways on proliferation, migration, and extracellular matrix production in a human lens cell line. *Exp Eye Res* 2011;**92**:173–9.
23. Goodpaster T, Legesse-Miller A, Harneed MR, Aisner SC, Randolph-Habecker J, Coller HA. An immunohistochemical method for identifying fibroblasts in formalin-fixed, paraffin-embedded tissue. *J Histochem Cytochem* 2008;**56**:347–58.

24. Pilling D, Fan T, Huang D, Kaul B, Gomer RH. Identification of markers that distinguish monocyte-derived fibrocytes from monocytes, macrophages, and fibroblasts. *Plos One* 2009;**4**:e7475.
25. Jansen DA, Graivier MH. Evaluation of a calcium hydroxylapatite-based implant (Radiesse) for facial soft-tissue augmentation. *Plast Reconstr Surg* 2006;**118**:22S–30S discussion 1S-3S.
26. Liu HH, Peng HJ, Wu Y, et al. The promotion of bone regeneration by nanofibrous hydroxyapatite/chitosan scaffolds by effects on integrin-BMP/Smad signaling pathway in BMSCs. *Biomaterials* 2013;**34**:4404–17.
27. Chen Z, Zhuo FL, Zhang SJ, Tian Y, Tian S, Zhang JZ. Modulation of tropoelastin and fibrillin-1 by infrared radiation in human skin in vivo. *Photodermatol Photoimmunol Photomed* 2009;**25**:310–16.
28. Mithieux SM, Weiss AS. Elastin. *Adv Protein Chem* 2005;**70**:437–61.
29. Yutskovskaya Y, Kogan E, Leshunov E. A randomized, split-face, histomorphologic study comparing a volumetric calcium hydroxylapatite and a hyaluronic acid-based dermal filler. *J Drugs Dermatol* 2014;**13**:1047–52.
30. Wang ZH, Zhang QS, Duan YL, Zhang JL, Li GF, Zheng DL. TGF-beta induced miR-132 enhances the activation of TGF-beta signaling through inhibiting SMAD7 expression in glioma cells. *Biochem Biophys Res Commun* 2015;**463**:187–92.
31. Magrez A, Kasas S, Salicio V, et al. Cellular toxicity of carbon-based nanomaterials. *Nano Lett* 2006;**6**:1121–5.
32. Parayanthala Valappil M, Santhakumar S, Arumugam S. Determination of oxidative stress related toxicity on repeated dermal exposure of hydroxyapatite nanoparticles in rats. *Int J Biomater* 2014;**2014**:476942.